agriculture

MDPI

Article

Long-Term Pepper (*Capsicum annuum* L.) Monoculture Reshapes Rhizosphere Soil Chemistry, Microbiota, and Metabolite Profiles

Fan Yang [1,†], Zihang Han [2,†], Ying Zhang [1], Xin Wang [1,3], Yuting Hong [1,3], Xiaoke Chang [1], Wenrui Yang [1], Yaxian Zhao [4,*] and Qiuju Yao [1,*]

[1] Institute of Vegetables, Henan Academy of Agricultural Sciences, Graduate Training and Research Base, Zhengzhou University, Zhengzhou 450002, China
[2] Institute of Plant Protection, Henan Academy of Agricultural Sciences, Zhengzhou 450002, China
[3] School of Agricultural Sciences, Zhengzhou University, Zhengzhou 450001, China
[4] Henan Provincial Center for Agricultural Product Quality and Safety and Green Food Development, Zhengzhou 450002, China
* Correspondence: 13603712766@163.com (Y.Z.); yaoqiuju@hnagri.org.cn (Q.Y.)
† These authors contributed equally to this work.

Abstract

Continuous monoculture alters rhizosphere soil conditions and microbial community structure, but the integrated soil biochemical, microbial, and metabolomic responses of pepper (*Capsicum annuum* L.) rhizosphere soils remain insufficiently characterized. Here, we compared uncropped/non-continuously cropped pepper soil (Y0) with soil under 10 years of pepper monoculture (Y10) using soil physicochemical assays, enzyme measurements, 16S rRNA and ITS amplicon sequencing, untargeted UHPLC-Q Exactive HFX metabolomics, and predictive functional profiling. Long-term monoculture markedly separated Y10 from Y0 in multivariate analyses. Y10 soils showed higher organic matter, available nitrogen, available phosphorus, available potassium, and electrical conductivity in soil-water extracts, whereas microbial biomass carbon and pH were lower. Soil enzyme profiles also differed between treatments. Microbial alpha diversity declined under Y10, and bacterial and fungal community structures were clearly separated between treatments. At the taxonomic level, Acidobacteriota and several oligotrophic bacterial taxa were relatively enriched in Y0, whereas Proteobacteria, Bacteroidota, Chloroflexi, Bacillota, *Pseudomonas*, *Bacillus*, and several fungal genus-level taxa increased in Y10. Untargeted metabolomics revealed extensive remodeling of rhizosphere metabolites, with 413 up-regulated and 21 down-regulated differential metabolites in Y10. Differential metabolites were mainly associated with carboxylic acids and derivatives, benzene and substituted derivatives, fatty acyls, aromatic-compound transformation, sulfur metabolism, alkaloid biosynthesis, and microbial metabolism. Correlation analyses further linked key microbial taxa with soil pH, microbial biomass carbon, available nutrients, electrical conductivity, and enzyme activities. These results indicate that long-term pepper monoculture is associated with coordinated shifts in soil chemical status, microbial community composition, and metabolite profiles. The study provides an integrated basis for understanding rhizosphere changes under pepper continuous-cropping systems while recognizing that functional predictions and metabolite annotations require experimental validation.

Keywords: *Capsicum annuum* L.; continuous-cropping obstacle; soil acidification; electrical conductivity; extracellular enzymes; 16S rRNA sequencing; ITS sequencing; PICRUSt2; FUNGuild; untargeted metabolomics

Academic Editors: Luciano Beneduce, Marko Petek, Aleksandra Perčin and Vladimir Zebec

Received: 15 June 2026
Revised: 17 July 2026
Accepted: 28 July 2026
Published: 1 August 2026

1. Introduction

Pepper (*Capsicum annuum* L.) is a high-value vegetable crop grown extensively in intensive production systems worldwide. Across major pepper-producing regions, limited arable land, the expansion of protected cultivation, and sustained market demand have driven repeated planting of the crop in the same fields. While continuous cropping streamlines field management in the short term, long-term monoculture frequently leads to soil degradation, elevated disease pressure, diminished plant vigor, and progressive yield decline. This phenomenon is widely termed continuous cropping obstacle or soil sickness [1,2]. Comparable issues have been documented across multiple horticultural crops, where continuous monoculture alters soil physicochemical properties, enzyme activities, nutrient cycling, and microbial community composition [2,3]. Accordingly, understanding how long-term pepper monoculture reshapes the rhizosphere environment is critical for developing sustainable strategies to alleviate cropping obstacles.

Rhizosphere microorganisms play a central role in plant nutrient acquisition, stress tolerance, and disease suppression [4,5]. Beneficial bacterial and fungal taxa can promote plant growth and inhibit pathogen proliferation, while pathogenic or opportunistic microbes tend to accumulate under repeated cultivation of the same host. Soil extracellular enzymes further mediate the biochemical conversion of organic matter and nutrients in the rhizosphere and are widely used as sensitive indicators of microbial metabolic activity and soil functional status [6,7]. Therefore, changes in enzyme activities under continuous cropping can provide an integrated signal of how repeated cultivation reshapes nutrient cycling processes and microbial functioning in soil. Previous studies on pepper systems have demonstrated that continuous cropping substantially alters bacterial and fungal community structure. Long-term chili monoculture has been shown to shift dominant rhizosphere microbial taxa and modify their associations with soil environmental variables [2]. In hot pepper soils, extended continuous cropping reduces bacterial diversity and network complexity, and alters predicted functions related to nitrogen, phosphorus, energy, amino acid, and carbohydrate metabolism [8]. Fungal communities are also highly responsive to pepper monoculture: long-term continuous cropping lowers soil pH and organic matter content, shifts the relative abundances of major fungal phyla including Mortierellomycota, Ascomycota, and Basidiomycota, increases the relative abundance of the plant-pathogenic genus *Fusarium*, and depletes beneficial fungi such as *Mortierella* and *Penicillium* [9]. These observations collectively suggest that shifts in both bacterial and fungal communities may contribute to the onset and progression of pepper continuous cropping obstacles.

Beyond soil properties and microbial communities, rhizosphere metabolites serve as a mechanistic link between plant roots and soil microorganisms. Root exudates and other rhizosphere metabolites can function as nutrient sources, chemical signals, allelochemicals, and antimicrobial compounds, thereby shaping microbial recruitment, pathogen suppression, and plant–soil feedbacks [10,11]. Experimental evidence has confirmed that root-exudate metabolites can drive plant–soil feedbacks by restructuring the rhizosphere microbiota [12]. In pepper, recent work further indicates that specific secondary metabolites such as flavonoids can simultaneously inhibit Phytophthora capsici and modulate the pepper rhizosphere microbiome [13]. These findings underscore the importance of examining rhizosphere metabolites in conjunction with microbial communities, rather than treating soil chemistry and microbiota as independent components.

Although previous studies have reported changes in pepper rhizosphere microbial communities under continuous cropping, most have focused on either bacterial/fungal composition or selected soil properties. The distinctive feature of the present study is the joint evaluation of soil physicochemical traits, extracellular enzyme activities, trace elements, bacterial and fungal communities, predicted microbial functions, and untar-

geted metabolite profiles from the same pepper production system. This design allowed us to evaluate whether long-term monoculture is associated with coordinated changes across soil chemistry, microbiota, and metabolic signatures rather than isolated shifts in individual indicators.

2. Materials and Methods

2.1. Experimental Site, Cropping Treatments, and Rhizosphere Soil Sampling

The experiment was conducted at a pepper seed-industry demonstration base in Shangguancao Village, Shixiang Town, Changge City, Xuchang, Henan Province, China (113°52′44″ E, 34°11′29″ N). The pepper cultivar was Qixuan 115. Rhizosphere soils were collected in June 2025 from two plots located within the same demonstration base. The Y0 plot represented a newly established pepper plot without a history of continuous pepper cropping, whereas the Y10 plot had been continuously cultivated with pepper for 10 years. The two plots had the same soil type and were managed under comparable fertilization and irrigation practices; the main treatment difference was the duration of pepper monoculture. Complete historical records of fertilizer inputs, pesticide applications, residue management, liming, and baseline soil properties before establishment of the Y10 system were not available, and this limitation is considered when interpreting the results.

Rhizosphere soil was collected from the main-root zone using an S-shaped sampling strategy. For each biological replicate, rhizosphere soils adhering to roots from five pepper plants were gently separated and homogenized to form one composite sample. The sampled plants were distributed along the S-shaped transect to reduce local spatial autocorrelation, although exact inter-plant distances were not recorded. Three biological replicates per group were used for soil physicochemical properties, enzyme activities, and mineral-element analyses, whereas six biological replicates per group were used for 16S rRNA/ITS amplicon sequencing and untargeted metabolomics. After sampling, rhizosphere soils were placed into cryotubes, immediately frozen in liquid nitrogen, transported to the laboratory on dry ice, and stored at −80 °C until molecular and metabolomic analyses. Subsamples for chemical assays were processed according to the requirements of each assay.

2.2. Soil Physicochemical Properties, Extracellular Enzyme Activities, and Mineral Elements

Soil physicochemical properties were determined using standard soil-analysis procedures. Soil organic matter (OM) was measured by potassium dichromate oxidation; microbial biomass carbon (MBC) was determined by the chloroform fumigation-extraction method [14,15]; available nitrogen (AN) was determined by alkaline hydrolysis diffusion [16]; available phosphorus (AP) was determined by molybdenum-antimony colorimetry; and available potassium (AK) was determined after ammonium acetate extraction. Soil pH and electrical conductivity (EC) were measured in soil-water extracts using a calibrated pH meter and conductivity meter, respectively [17,18]. Instrument calibration and quality-control procedures followed the testing laboratory's standard operating protocols.

Four extracellular enzyme activities were quantified because they represent key microbial and nutrient-cycling processes in soil: dehydrogenase (S-DHA) for microbial oxidative activity, acid phosphatase (S-ACP) for phosphorus cycling, urease (S-URE) for nitrogen transformation, and sucrase/invertase (S-SUC) for carbon turnover. S-URE activity was assayed using urea as the substrate; S-DHA activity was measured using triphenyltetrazolium chloride reduction; S-ACP activity was measured using disodium phenyl phosphate as the substrate; and S-SUC activity was determined using sucrose as the substrate. Enzyme activities were calculated on a dry-soil-mass basis and expressed as U g-1 soil according to the assay definitions used by the testing laboratory.

Soil Ca, Mg, Fe, Zn, and Cu contents were determined after complete digestion of air-dried soil samples using a mixed-acid digestion procedure suitable for total mineral-element determination [19–21]. Digested solutions were brought to a fixed volume with ultrapure water, filtered when necessary, and analyzed using calibrated elemental-analysis instrumentation. Blank samples and standard solutions were included for quality control.

2.3. DNA Extraction, Amplicon Library Construction, and Sequencing

Total soil DNA was extracted from rhizosphere soil using the TIANamp Soil DNA Kit (DP336; TIANGEN Biotech (Beijing) Co., Ltd., Beijing, China) according to the manufacturer's instructions. DNA quality was assessed using agarose gel electrophoresis and spectrophotometry; DNA samples with an A260/A280 ratio greater than 1.5, as determined by NanoDrop (Thermo Fisher Scientific, Waltham, MA, USA), were used for library construction. The bacterial 16S rRNA V3-V4 region was amplified using primers 341F (5′-CCTACGGGNGGCWGCAG-3′) and 806R (5′-GACTACHVGGGTATCTAATCC-3′). The fungal ITS2 region was amplified using the ITS3/ITS4 primer pair ITS3 (5′-GCATCGATGAAGAACGCAGC-3′) and ITS4 (5′-TCCTCCGCTTATTGATATGC-3′). Amplicon libraries were sequenced on an Illumina platform (Illumina Inc., San Diego, CA, USA) by the sequencing service provider.

2.4. Amplicon Sequence Processing, Taxonomic Annotation, Diversity Analysis, and Functional Prediction

Raw paired-end reads were quality-filtered using Trimmomatic v0.36 and PEAR v0.9.6 [22,23]. Reads were trimmed using a 50 bp sliding window with an average quality threshold of Q20; reads shorter than 120 bp or containing ambiguous bases were discarded. Paired-end reads were merged using FLASH v1.20 and PEAR v0.9.6, with a minimum overlap length of 10 bp and a maximum mismatch rate of 0.1 [23,24]. Barcodes and primer sequences were trimmed, and chimeric sequences were filtered out using VSEARCH v2.7.1 [25]. All subsequent bioinformatic processing was performed using the QIIME2 pipeline (version 2019.7), and high-quality sequences were clustered into operational taxonomic units (OTUs) at 97% sequence similarity using a UPARSE/VSEARCH-based workflow [25,26]. This OTU-based approach was chosen to maintain consistency with the service provider's original analysis workflow and to ensure direct compatibility with the STAMP differential-abundance tables used in this study; although amplicon sequence variant (ASV) approaches can provide higher nucleotide-level resolution, the OTU-based workflow enables direct comparison with the precomputed taxonomic and functional outputs provided by the sequencing service. For taxonomic assignment, a uniform confidence threshold of 0.7 was applied: representative bacterial 16S rRNA gene sequences were annotated against the SILVA SSU rRNA database (Release 138.1) [27], and representative fungal ITS sequences were annotated against the UNITE database [28]. Taxonomic composition was summarized at the phylum and genus levels for subsequent analysis.

Alpha diversity was assessed using the observed OTUs and Shannon indices. For beta diversity, principal coordinate analysis (PCoA) based on the distance matrix generated by the sequencing analysis pipeline was constructed to visualize the differences in microbial community structure between the Y0 and Y10 groups. Given that this study involved only two field conditions from a single demonstration base, the PCoA patterns were interpreted as descriptive evidence of community separation rather than definitive proof of causal treatment effects. Differentially abundant taxa between the two cropping regimes were identified via nonparametric statistical analysis, and the differences in relative abundance were visualized using STAMP-style comparisons [29]. For functional inference, bacterial functional profiles were predicted from 16S rRNA gene data using PICRUSt2 with annota-

tion against KEGG pathways [30,31], while fungal functional guilds were assigned based on ITS sequence data using FUNGuild [32].

2.5. Untargeted Metabolomic Profiling of Rhizosphere Soil

Untargeted metabolomic profiling was conducted with six biological replicates per group. For each sample, approximately 50 mg of rhizosphere soil was weighed into a centrifuge tube, and 400 μL of 70% methanol extraction solution containing internal standards was added. Samples were vortexed for 3 min, sonicated in an ice-water bath for 10 min, vortexed again for 1 min, and incubated at −20 °C for 30 min. After centrifugation at 12,000 rpm and 4 °C for 10 min, the supernatant was collected and subjected to a second centrifugation step at 12,000 rpm and 4 °C for 3 min. The final supernatant was transferred to sample vials for instrumental analysis.

Quality control samples were prepared by pooling equal aliquots from all samples and were injected at regular intervals throughout the analytical run to monitor instrument stability and data reproducibility. Chromatographic separation was performed using an ultra-high-performance liquid chromatography system coupled to a Q Exactive HFX mass spectrometer (UHPLC-Q Exactive HFX; Thermo Fisher Scientific, Waltham, MA, USA). Separation was achieved using a Waters ACQUITY Premier HSS T3 column (Waters Corp., Milford, MA, USA). The mobile phase consisted of 0.1% formic acid in water (phase A) and 0.1% formic acid in acetonitrile (phase B). The column temperature was maintained at 40 °C, the flow rate was set to 0.4 mL min^{-1}, and the injection volume was 4 μL. Mass spectrometric data were acquired in both positive and negative electrospray ionization modes.

Untargeted metabolomics analysis was performed using a UHPLC-Q Exactive HFX platform (Thermo Fisher Scientific, Waltham, MA, USA). Raw mass spectrometry data were converted to mzXML format using ProteoWizard (version 3.0) and processed with XCMS R package (version 3.8.3, Bioconductor 3.10) for peak extraction, peak alignment, and retention time correction [33,34]; peak areas were further corrected for signal drift, subjected to normalization, and features with more than 50% missing values within each group were excluded from downstream analysis. Quality-control samples were used throughout the analytical run to monitor instrument stability and analytical reproducibility. Metabolite annotation was conducted by matching accurate mass, retention time, isotope patterns, and MS/MS fragmentation information against in-house and public metabolite databases, with additional support from reaction-network-based annotation strategies where appropriate [35]; the KEGG and HMDB databases were employed for metabolite pathway annotation and chemical classification [36], and unless confirmed by authentic reference standards, all metabolite identifications were considered putative annotations. Differential metabolites between the Y0 and Y10 groups were screened using combined thresholds: variable importance in projection (VIP) > 1 derived from the multivariate model, fold change > 1.5 or <1/1.5, and $p < 0.05$. Finally, KEGG pathway enrichment analysis was performed to identify metabolic pathways altered by continuous cropping and to prioritize pathways that may be closely linked to soil microbial metabolism.

2.6. Statistical Analysis and Visualization

All statistical analyses were performed using R (version 4.4.1) and associated packages unless otherwise specified. Before two-group comparisons, the normality of residuals and homogeneity of variance were assessed using Shapiro–Wilk and Levene-type tests where applicable. Soil physicochemical properties, enzyme activities, and mineral elements were compared between Y10 and Y0 using Student's *t*-test when assumptions were met. For amplicon and metabolomic analyses, *p*-values and corrected values were

interpreted according to the output of each analysis pipeline. Spearman correlation analysis was used to explore associations among soil variables and key microbial genus-level taxa. Because soil properties were measured using three biological replicates per group whereas sequencing used six biological replicates per group, correlation heatmaps should be interpreted as exploratory associations rather than as confirmatory evidence of direct microbial-environmental interactions.

Microbial alpha diversity, beta diversity, taxonomic composition, differentially abundant taxa, functional prediction profiles, and metabolomic data were analyzed following the corresponding bioinformatic and metabolomic workflows described above. Spearman correlation analysis was performed to assess associations between key bacterial or fungal genera and soil physicochemical variables, enzyme activities, and mineral elements. Hierarchical clustering was applied to both microbial taxa and environmental variables for the correlation heatmaps. Figures were generated using R (version 4.4.1)-based visualization workflows, including the ggplot2 package where applicable [37,38].

3. Results

3.1. Long-Term Continuous Cropping Altered Soil Nutrient Status, Salinity, pH, and Biological Activity

Long-term pepper monoculture was associated with broad shifts in soil physicochemical properties and enzyme activities (Figure 1 and Supplementary Table S1). PCA based on soil phenotypic indicators separated Y10 from Y0 primarily along PC1, which explained 88.4% of the total variation (Figure 1A). Hierarchical clustering of extracellular enzyme activities also grouped samples according to cropping history, indicating distinct enzyme-activity profiles between Y0 and Y10 (Figure 1B).

Compared with Y0, Y10 soils had higher OM, AN, AP, AK, and EC values, whereas MBC and pH were lower (Figure 1C). The increase in EC refers to electrical conductivity measured in soil-water extracts and is therefore described as an indicator of higher soluble-ion concentration rather than direct evidence of salinity stress. Mineral element patterns showed lower Ca, Mg, Fe, Zn, and Cu contents in Y10 than in Y0 (Figure 1D).

Together, these results show that the 10-year monoculture system differed from the non-continuously cropped system in soil acidity, microbial biomass, nutrient availability, EC, mineral elements, and enzyme profiles.

3.2. The Rhizosphere Metabolome Was Pronouncedly Reprogrammed After 10 Years of Continuous Cropping

Untargeted metabolomics revealed pronounced differences in rhizosphere metabolite profiles between Y0 and Y10 (Figure 2). Metabolite-class annotation showed that the detected features were mainly assigned to carboxylic acids and derivatives, benzene and substituted derivatives, fatty acyls, organooxygen compounds, organo-nitrogen compounds, prenol lipids, indoles and derivatives, pyridines and derivatives, and related classes (Figure 2A).

Principal component analysis of metabolomic profiles separated most Y10 samples from Y0 samples, indicating that long-term monoculture was associated with a distinct rhizosphere metabolite composition (Figure 2B). Differential-metabolite screening identified 434 differential metabolites, including 413 metabolites with higher abundance in Y10 and 21 metabolites with lower abundance in Y10 relative to Y0 (Figure 2C).

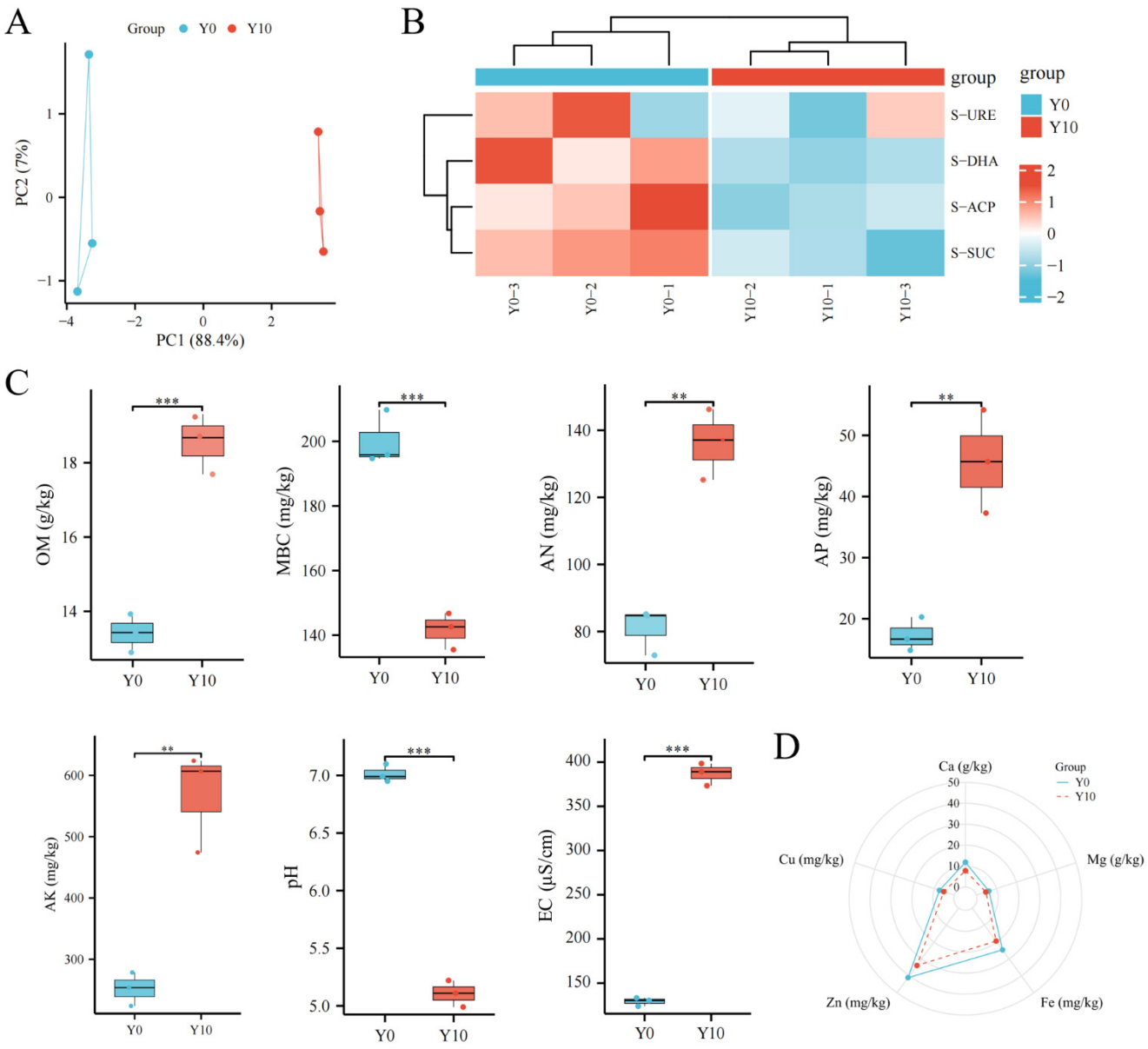

Figure 1. Effects of long-term pepper monoculture on rhizosphere soil properties and enzyme activities. (**A**) Principal component analysis (PCA) of soil physicochemical, enzyme, and element indicators. (**B**) Hierarchical clustering heatmap of extracellular enzyme activities. (**C**) Boxplots of OM, MBC, AN, AP, AK, pH, and EC. (**D**) Radar plot of Ca, Mg, Fe, Zn, and Cu. Soil physicochemical, enzyme, and element analyses were performed with three biological replicates per group (n = 3). Asterisks indicate significant differences between Y0 and Y10 based on t-tests (** $p < 0.01$, *** $p < 0.001$).

The heatmap of differential metabolites showed clear treatment-related clustering, with most differential features showing higher relative abundance in Y10 than in Y0 (Figure 2D). Among the metabolites with the largest positive log2 fold changes were vildagliptin, 3,4,3,4-bis(O,O-methylene)ellagic acid-related features, crambescidin 359, and several aromatic or heterocyclic compounds. Metabolites with the strongest negative log2 fold changes included clozapine, quinolinone-related compounds, octyl gallate, hypodemapyrazine, and related features (Figure 2E and Supplementary Table S2). These metabolite names are reported according to database annotations and should be considered putative unless confirmed by authentic standards.

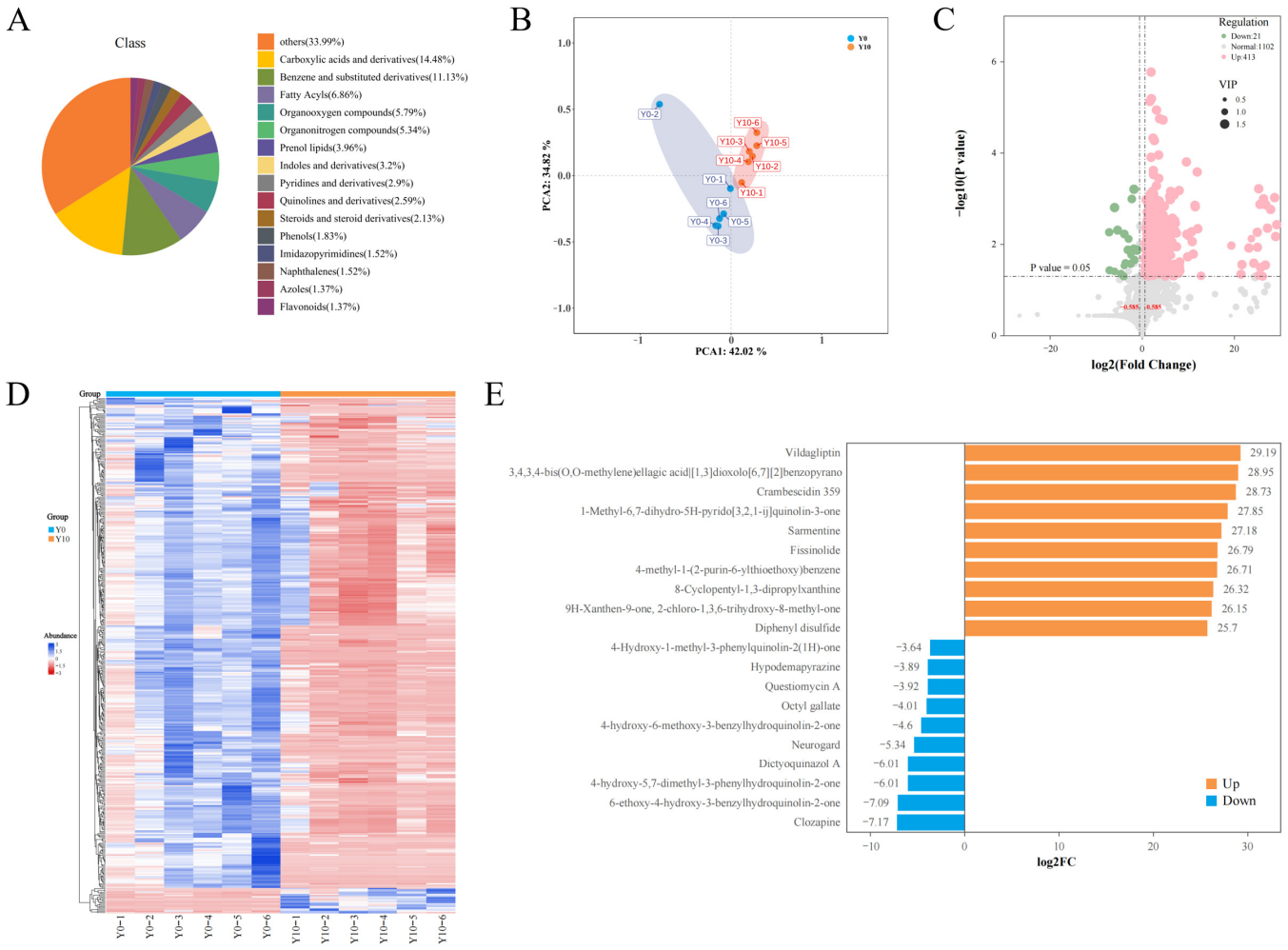

Figure 2. Untargeted metabolomic profiling of pepper rhizosphere soils under Y0 and Y10 conditions. (**A**) Chemical-class distribution of annotated metabolites. (**B**) PCA score plot of metabolomic profiles. (**C**) Volcano plot of differential metabolites. (**D**) Heatmap of differential metabolites. (**E**) Top differential metabolites ranked by log2 fold change. Untargeted metabolomics was performed with six biological replicates per group (n = 6).

3.3. KEGG Enrichment Linked Continuous-Cropping-Responsive Metabolites to Microbial and Aromatic Compound Metabolism

To further examine the functional context of altered metabolites, KEGG pathway analysis was performed for differential metabolites between Y10 and Y0 (Figure 3). Pathway ranking highlighted microbial metabolism in diverse environments, degradation of aromatic compounds, biosynthesis of alkaloids derived from shikimate, indole alkaloid biosynthesis, sulfur metabolism, caffeine metabolism, oxidative phosphorylation, biosynthesis of terpenoids and steroids, and xenobiotic-related pathways (Figure 3A).

A heatmap of representative metabolites from these candidate pathways showed treatment-dependent abundance patterns (Figure 3B). Several aromatic compounds and secondary metabolites, including benzene, ethylbenzene, benzaldehyde, 4-hydroxybenzaldehyde, 4-hydroxyphenyl acetate, allantoin-related compounds, DOPA, dictamnine, and fumaric acid, contributed to the separation between Y0 and Y10. These results suggest that long-term pepper monoculture was associated with broad changes in pathways related to microbial metabolism and secondary-metabolite turnover.

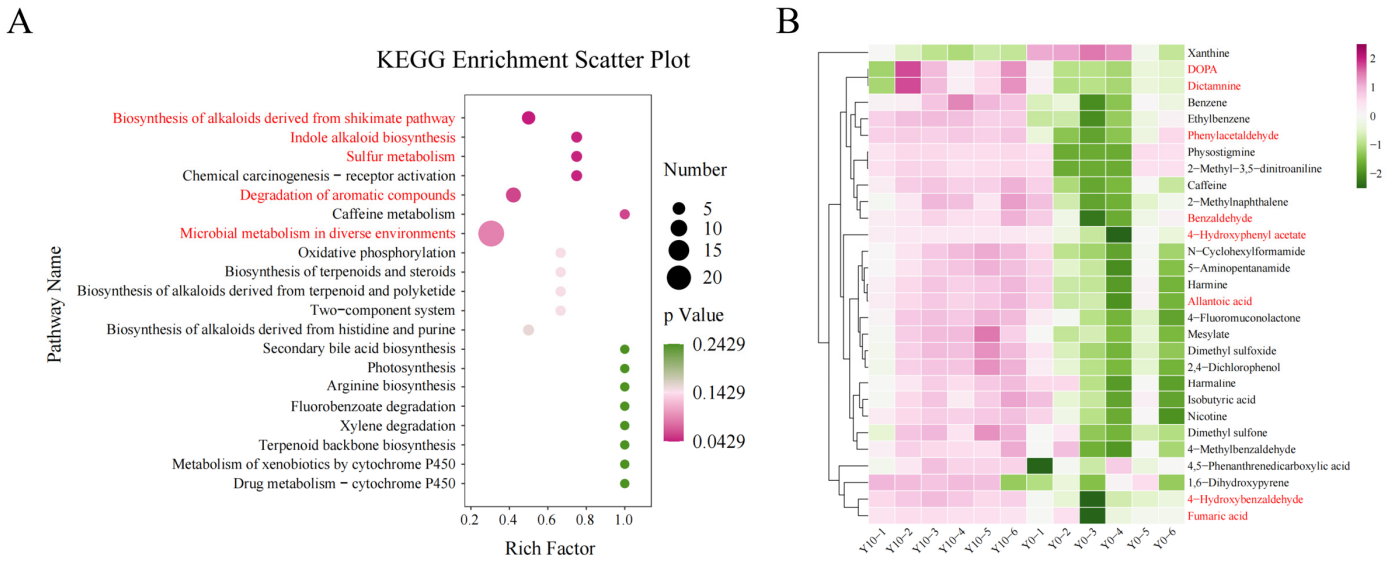

Figure 3. KEGG pathway analysis and candidate metabolite patterns of differential metabolites. (**A**) KEGG pathway scatter plot showing pathway ranking by rich factor, metabolite number, and *p*-value. Red labels indicate candidate pathways selected for further visualization. (**B**) Heatmap of representative differential metabolites from selected pathways. Six biological replicates per group were used ($n = 6$). Perform a KEGG pathway enrichment analysis, sort the results by *p*-value, and select the top 20 pathways with the lowest *p*-values to create a bubble plot.

Together, the KEGG enrichment and selected-metabolite heatmap showed that the metabolomic shift induced by long-term continuous cropping was not restricted to a single compound class. Instead, the response involved multiple pathways associated with microbial metabolism, aromatic compound transformation, sulfur metabolism, and secondary metabolite biosynthesis.

3.4. Bacterial and Fungal Diversity Declined Under Continuous Cropping and Was Accompanied by Distinct Community Separation

Amplicon sequencing showed that long-term pepper monoculture was associated with reduced microbial richness and diversity and with clear shifts in bacterial and fungal community structure (Figure 4 and Supplementary Table S3). For bacteria, the Venn diagram showed 3965 shared OTUs between Y0 and Y10, with 1820 unique to Y0 and 1026 unique to Y10 (Figure 4A). Observed OTUs and Shannon diversity were both lower in Y10 than in Y0 (Figure 4B). The bacterial PCoA showed a clear separation between Y0 and Y10 along PCoA1, which explained 70.15% of the variation, while PCoA2 explained 8.48% (Figure 4C and Supplementary Table S3).

For fungi, 346 OTUs were shared between Y0 and Y10, with 423 unique to Y0 and 153 unique to Y10 (Figure 4D). Fungal observed OTUs and Shannon diversity were also lower in Y10 than in Y0 (Figure 4E). The fungal PCoA separated Y10 from Y0 along PCoA1, which explained 56.24% of the variation, while PCoA2 explained 11.00% (Figure 4F and Supplementary Table S3). These patterns indicate that long-term monoculture was associated with lower within-sample diversity and altered between-sample community structure in both bacterial and fungal assemblages.

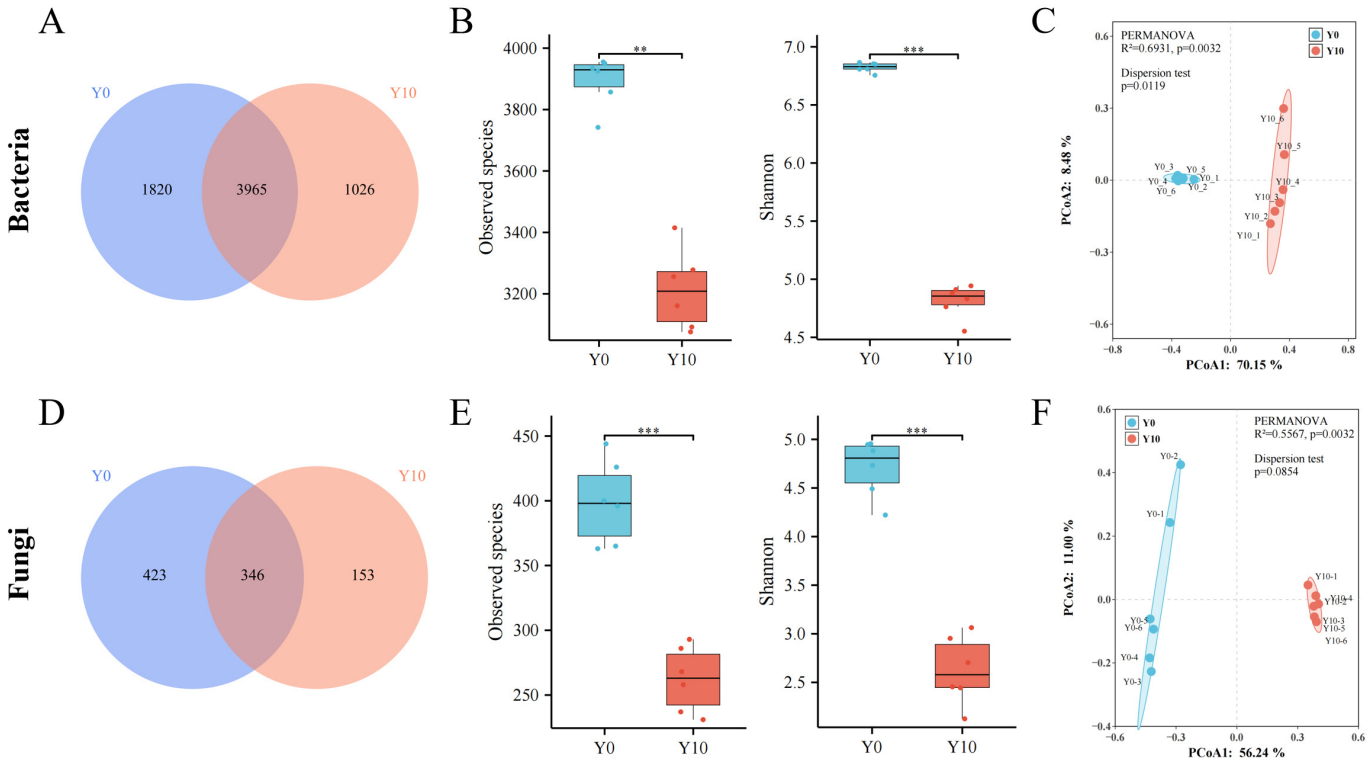

Figure 4. Alpha and beta diversity of bacterial and fungal communities in pepper rhizosphere soils. (**A**) Bacterial Venn diagram. (**B**) Bacterial observed OTUs and Shannon diversity. (**C**) Bacterial PCoA. (**D**) Fungal Venn diagram. (**E**) Fungal observed OTUs and Shannon diversity. (**F**) Fungal PCoA. Amplicon sequencing was performed with six biological replicates per group (n = 6). Asterisks indicate significant differences between Y0 and Y10 (** $p < 0.01$, *** $p < 0.001$).

3.5. Continuous Cropping Changed the Dominant Bacterial and Fungal Taxa in Pepper Rhizosphere Soil

The relative-abundance profiles showed distinct changes in bacterial and fungal taxonomic composition under long-term monoculture (Figure 5). At the bacterial phylum level, Proteobacteria, Acidobacteriota, Chloroflexi, Bacteroidota, Actinobacteriota, Gemmatimonadota, Patescibacteria, Myxococcota, and Bacillota (formerly Firmicutes) were the dominant groups (Figure 5A). Compared with Y0, Y10 showed a higher relative abundance of Proteobacteria, Bacteroidota, Chloroflexi, Patescibacteria, and Bacillota, whereas Acidobacteriota and several other groups were relatively lower.

At the bacterial genus or genus-level taxon level, *RB41*, *Pseudomonas*, *LWQ8*, *Nitrospira*, *Steroidobacter*, *A4b*, *Bacillus*, and other taxa contributed substantially to the community composition (Figure 5B). *RB41*, *Nitrospira*, *Bryobacter*, and several Acidobacteriota-related genus-level taxa were more abundant in Y0, whereas *Pseudomonas*, *Bacillus*, *A4b*, *LWQ8*, *AKYG1722*, and selected other taxa were more abundant in Y10.

At the fungal phylum level, Ascomycota was the dominant phylum in both groups, followed by uncultured fungi, Mortierellomycota, Chytridiomycota, Basidiomycota, and other low-abundance phyla (Figure 5C). Y10 showed a higher relative abundance of Ascomycota and Chytridiomycota but a lower relative abundance of Mortierellomycota than Y0. At the fungal genus or genus-level taxon level, major taxa included *Botryotrichum*, *Chaetomium*, *Cephalophora*, *Ascolobus*, *Alternaria*, *Fusarium*, *Aspergillus*, *Iodophanus*, and related taxa (Figure 5D). Several taxa, including *Botryotrichum*, *Fusarium*, *Aspergillus*, *Alternaria*, and other genus-level taxa that contain species with saprotrophic, opportunistic, or plant-associated lifestyles, showed higher relative abundance in Y10, whereas unidentified Pyronemataceae genera and Mortierella-related taxa were more abundant in Y0.

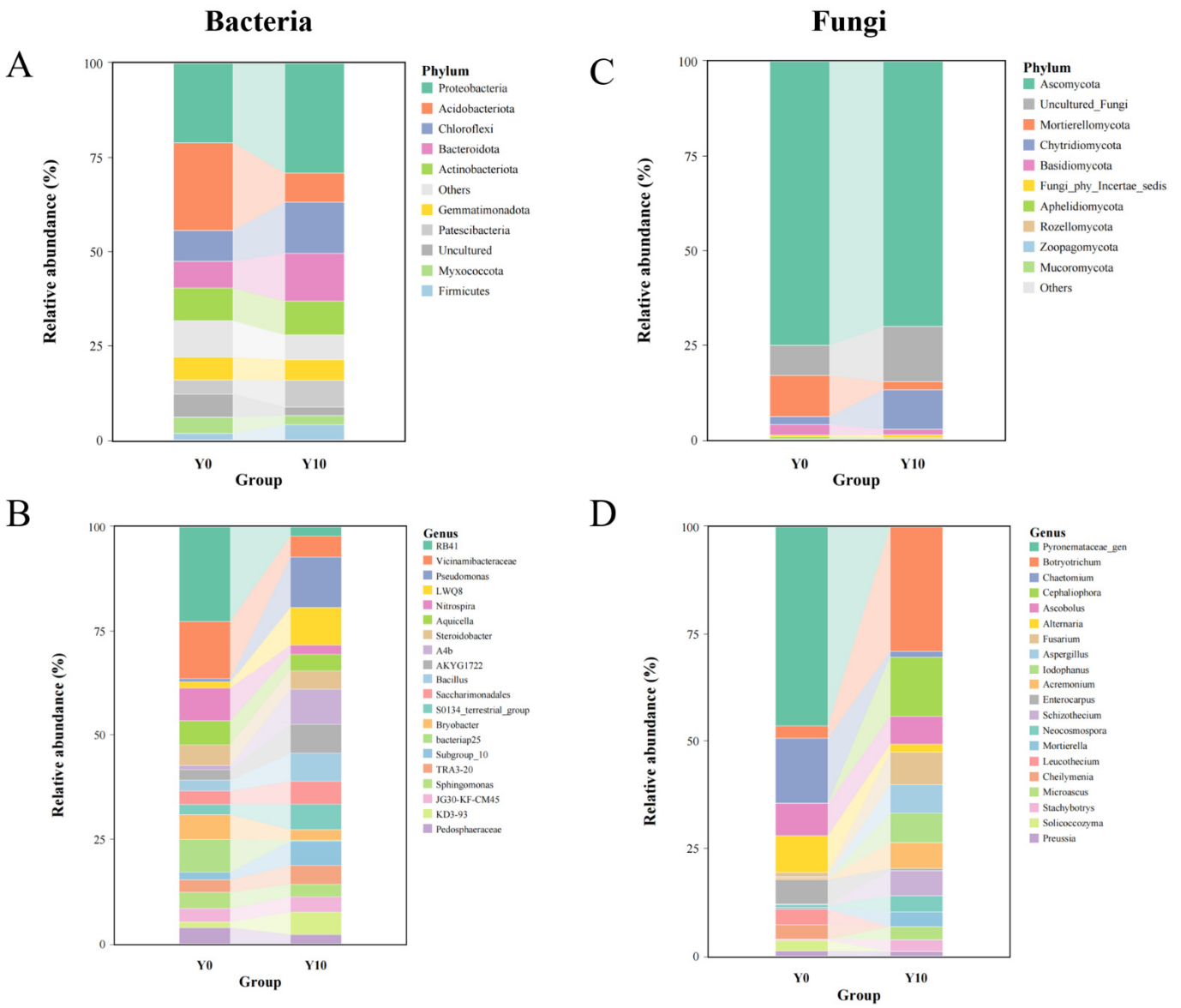

Figure 5. Relative abundance of bacterial and fungal taxa in pepper rhizosphere soils. (**A**) Bacterial phylum-level composition. (**B**) Bacterial genus or genus-level taxon composition. (**C**) Fungal phylum-level composition. (**D**) Fungal genus or genus-level taxon composition. Values are group mean relative abundances based on six biological replicates per group (n = 6). Genus-level labels include formally named genera and unresolved genus-level taxa.

3.6. Differential Taxa Revealed Continuous-Cropping-Associated Microbial Signatures

Non-parametric differential-abundance analysis further identified taxa that differed between Y0 and Y10 (Figure 6). At the bacterial phylum level, Acidobacteriota, uncultured bacteria, Nitrospirota, Myxococcota, and Methylomirabilota were higher in Y0, whereas Proteobacteria, Bacteroidota, Chloroflexi, Patescibacteria, and Bacillota were higher in Y10 (Figure 6A).

At the bacterial genus or genus-level taxon level, *RB41*, *bacteria25*, *Nitrospira*, *Bryobacter*, *Subgroup 25*, *Subgroup 7*, *SWB02*, and *AKAU4049* were higher in Y0, whereas *Pseudomonas*, *LWQ8*, *A4b*, *AKYG1722*, *Chryseolinea*, *Bacillus*, *Subgroup 10*, *S0134* terrestrial group, and *Algoriphagus* were higher in Y10 (Figure 6B).

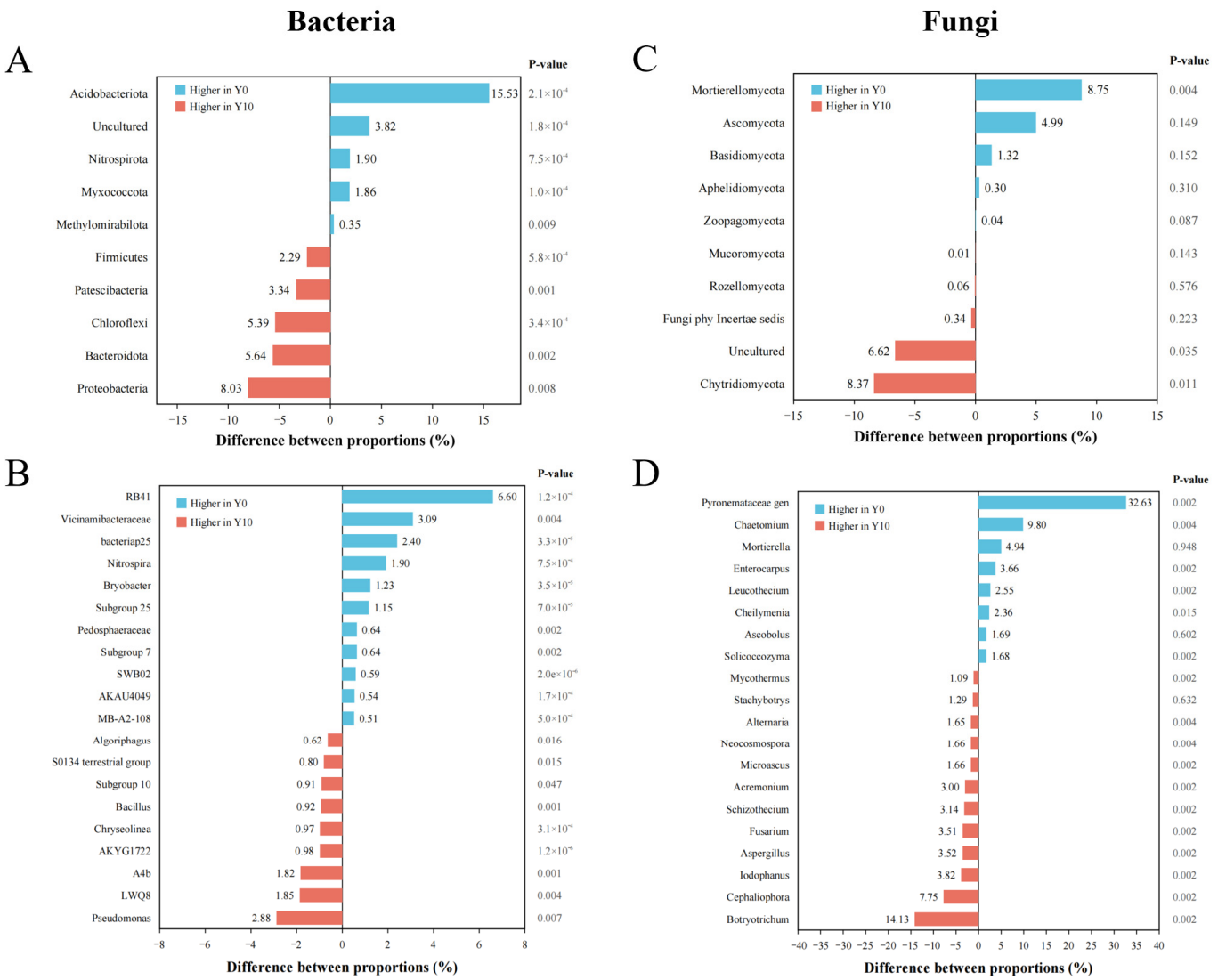

Figure 6. Differential-abundance analysis of bacterial and fungal taxa between Y0 and Y10. (**A**) Bacterial phyla. (**B**) Bacterial genus or genus-level taxa. (**C**) Fungal phyla. (**D**) Fungal genus or genus-level taxa. Bars indicate the difference between group proportions; blue bars indicate higher relative abundance in Y0, and red bars indicate higher relative abundance in Y10. *p*-values are shown next to each taxon according to the STAMP output. Six biological replicates per group were used ($n = 6$).

For fungi, Mortierellomycota, Ascomycota, Basidiomycota, Aphelidiomycota, and Zoopagomycota were higher in Y0, whereas Chytridiomycota was higher in Y10 (Figure 6C). At the fungal genus or genus-level taxon level, *Chaetomium*, *Mortierella*, *Enterocarpus*, *Leucothecium*, *Cheilymenia*, *Ascolobus*, and *Solicoccozyma* were higher in Y0, whereas *Botryotrichum*, *Cephalophora*, *Iodophanus*, *Aspergillus*, *Fusarium*, *Schizothecium*, *Acremonium*, *Microascus*, *Neocosmospora*, *Alternaria*, *Stachybotrys*, and *Mycothermus* were higher in Y10 (Figure 6D). These results identify the taxa most strongly associated with long-term monoculture, but they do not establish pathogenicity or functional roles.

At the fungal genus level, unidentified Pyronemataceae genera showed the largest Y0-associated difference, with a difference between proportions of 32.63% ($p = 0.002$; Figure 6D). *Chaetomium*, *Enterocarpus*, *Leucothecium*, *Cheilymenia*, and *Solicoccozyma* were also significantly more abundant in Y0. *Mortierella* and *Ascobolus* showed higher mean proportions in Y0, but their differences were not significant. In contrast, *Botryotrichum* was the most strongly enriched fungal genus in Y10, with a difference of 14.13% ($p = 0.002$). *Cephaliophora*, *Iodophanus*, *Aspergillus*, *Fusarium*, *Schizothecium*, *Acremonium*, *Microascus*, *Neo-*

cosmospora, *Alternaria*, and *Mycothermus* were also significantly enriched in Y10. Together, these differential taxa indicate that long-term continuous cropping selected for distinct bacterial and fungal assemblages, with Y10 characterized by enrichment of several bacterial genera such as *Pseudomonas* and *Bacillus* and fungal genera including *Botryotrichum*, *Fusarium*, *Aspergillus*, *Neocosmospora*, and *Cephaliophora*.

3.7. Predicted Microbial Functions Shifted Toward Transport, Degradation, and Pathogen-Associated Fungal Guilds Under Continuous Cropping

Predictive functional profiling was used to explore potential functional differences associated with the bacterial and fungal communities (Figure 7). PICRUSt2-based KEGG pathway prediction indicated that pathways including lipopolysaccharide biosynthesis, biosynthesis of vancomycin-group antibiotics, betalain biosynthesis, thiamine metabolism, branched-chain amino-acid biosynthesis, selenocompound metabolism, lipoic-acid metabolism, and aminoacyl-tRNA biosynthesis were predicted to be higher in Y0 (Figure 7A). In contrast, bacterial chemotaxis, synthesis and degradation of ketone bodies, geraniol degradation, caprolactam degradation, ABC transporters, limonene and pinene degradation, and flagellar assembly were predicted to be higher in Y10.

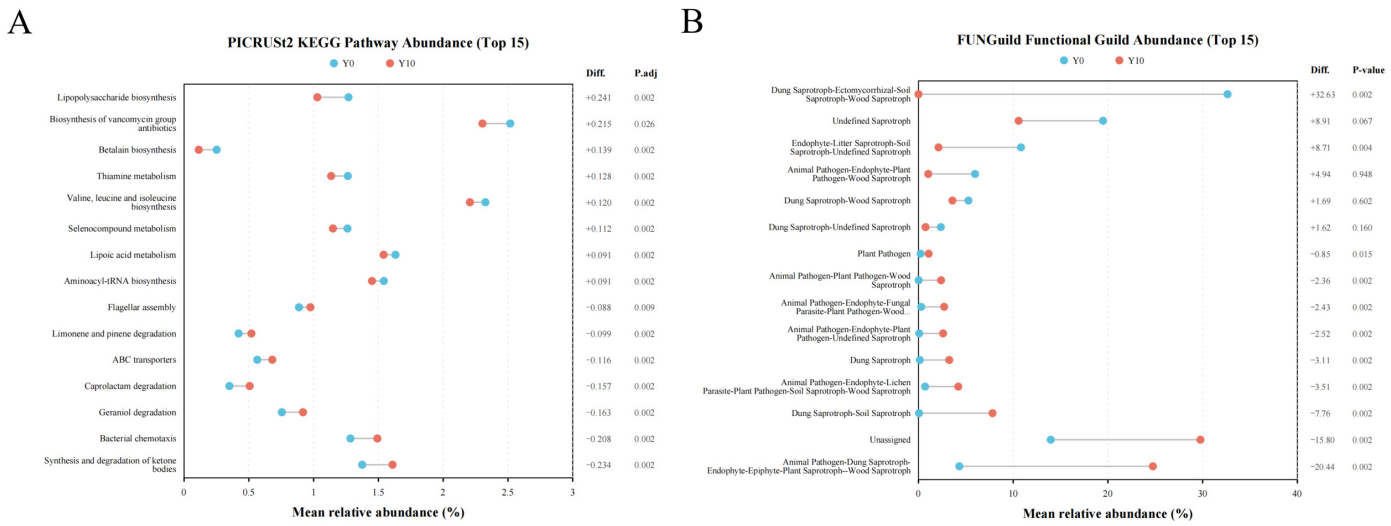

Figure 7. Predicted bacterial and fungal functional profiles. (**A**) PICRUSt2-predicted KEGG pathway abundance. (**B**) FUNGuild-predicted fungal functional guild abundance. Points indicate group mean relative abundance; lines connect Y0 and Y10 values for the same pathway or guild. Six biological replicates per group were used for amplicon sequencing (n = 6). Feature predictions represent potential features only.

FUNGuild-based prediction indicated that several saprotrophic or mixed trophic guilds differed between groups (Figure 7B). Guilds with higher predicted abundance in Y0 included dung saprotroph-ectomycorrhizal-soil saprotroph-wood saprotroph, undefined saprotroph, and endophyte-litter saprotroph-soil saprotroph-undefined saprotroph. Several plant-pathogen- or animal-pathogen-associated mixed guilds, dung saprotroph-soil saprotroph, unassigned guilds, and complex mixed guilds were higher in Y10. Because FUNGuild predictions are based on taxonomic assignment and guild databases, these results should be regarded as functional potential, and mixed or unassigned guilds should be interpreted cautiously.

Fungal functional guild prediction using FUNGuild also revealed clear differences between Y0 and Y10 (Figure 7B). Several saprotrophic or mixed trophic guilds were more abundant in Y0. The largest Y0-associated difference was observed for the dung saprotroph-ectomycorrhizal-soil saprotroph-wood saprotroph guild, which was 32.63% higher in

Y0 than in Y10 (p = 0.002). The endophyte-litter saprotroph-soil saprotroph-undefined saprotroph guild was also significantly higher in Y0 (difference = 8.71%, p = 0.004), while undefined saprotroph and other saprotrophic guilds showed higher mean abundance in Y0 but were not all statistically significant.

3.8. Soil Environmental Gradients Were Closely Associated with Key Bacterial and Fungal Genera

Spearman correlation analysis was used to explore associations between key genus-level taxa and soil variables (Figure 8). For bacteria, taxa that were higher in Y10, including *Pseudomonas*, *Bacillus*, *A4b*, *Chryseolinea*, *AKYG1722*, *LWQ8*, and the *S0134* terrestrial group, tended to correlate positively with AP, AK, EC, OM, and AN and negatively with MBC, pH, Ca, Mg, and several enzyme activities (Figure 8A). In contrast, taxa higher in Y0, including *RB41*, *Bryobacter*, *bacteria25*, *SWB02*, *Subgroup 25*, *AKAU4049*, *Nitrospira*, and related genus-level taxa, showed the opposite pattern.

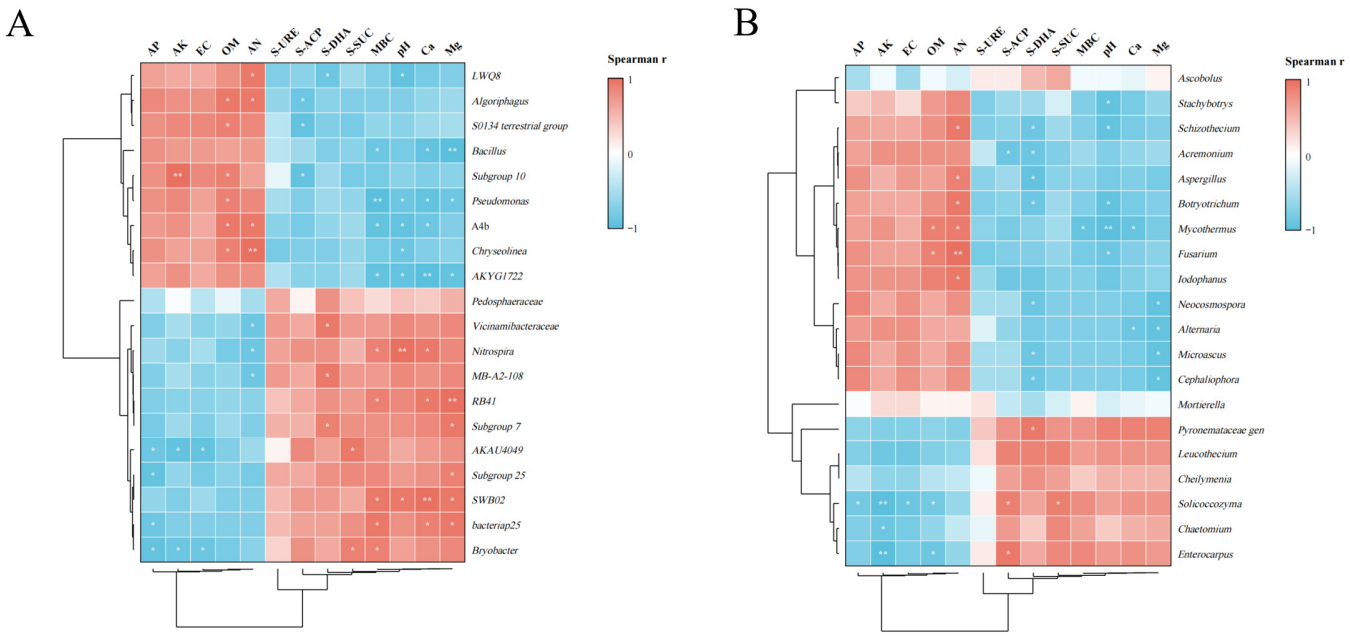

Figure 8. Spearman correlation heatmaps linking key microbial genus-level taxa with soil physicochemical properties and enzyme activities. (**A**) Bacterial genus-level taxa. (**B**) Fungal genus-level taxa. Red indicates positive correlations and blue indicates negative correlations. Asterisks indicate nominal significance levels from Spearman correlation analysis. Because soil variables were measured with three biological replicates per group and sequencing was performed with six biological replicates per group, these correlations should be interpreted as exploratory associations. Asterisks indicate significant correlations: * $p < 0.05$, ** $p < 0.01$.

For fungi, several Y10-associated genus-level taxa, including *Botryotrichum*, *Fusarium*, *Aspergillus*, *Acremonium*, *Schizothecium*, *Microascus*, *Neocosmospora*, *Alternaria*, and *Cephalophora*, tended to correlate positively with AP, AK, EC, OM, and AN but negatively with S-URE, S-ACP, S-DHA, S-SUC, MBC, pH, Ca, and Mg (Figure 8B). In contrast, Y0-associated taxa, including *Leucothecium*, *Cheilymenia*, *Solicoccozyma*, *Chaetomium*, and *Enterocarpus*, showed positive correlations with MBC, pH, Ca, Mg, and enzyme activities and negative correlations with AP, AK, EC, OM, and AN. These correlation patterns are exploratory and should not be interpreted as evidence of direct causation.

Fungal genera showed a similarly structured correlation pattern (Figure 8B). Several Y10-associated fungal genera, including *Schizothecium*, *Acremonium*, *Aspergillus*, *Botryotrichum*, *Mycothermus*, *Fusarium*, *Iodophanus*, *Neocosmospora*, *Alternaria*, *Microascus*, and *Cephaliophora*, were positively correlated with AP, AK, EC, OM, and AN. These genera

were negatively correlated with soil enzyme activities, MBC, pH, Ca, and Mg. *Fusarium*, *Aspergillus*, *Neocosmospora*, *Cephaliophora*, and *Botryotrichum* showed particularly consistent positive associations with the nutrient- and salinity-enriched conditions observed in Y10.

4. Discussion

Long-term pepper monoculture was associated with a distinctive soil chemical profile characterized by lower pH and MBC but higher OM, available nutrients, and EC in soil-water extracts. These patterns are consistent with the accumulation of fertilizer-derived nutrients and soluble ions under intensive cultivation, but the present field comparison cannot separate monoculture duration from the cumulative effects of fertilization history and other long-term management inputs.

One noteworthy feature of our results was the increase in OM in Y10 soils. This pattern differs from some long-term pepper continuous-cropping studies in which soil OM declined with increasing cropping years [9]. However, OM accumulation under continuous cropping can occur when fertilization, crop residue input, or root-derived carbon deposition exceeds microbial decomposition. In our study, higher OM in Y10 occurred together with lower MBC and reduced enzyme activities, implying that the accumulated organic matter may have been less efficiently transformed into microbial biomass. Therefore, the increase in OM should not be interpreted as an improvement in soil health. Rather, it may reflect an imbalance between carbon input and microbial turnover under acidified and high-EC conditions. This interpretation is supported by studies in garlic and other continuous-cropping systems, where acidification and altered enzyme activities were closely linked to microbial community deterioration and cropping obstacles [3].

The untargeted metabolomics results further indicate that long-term pepper continuous cropping strongly altered the rhizosphere chemical environment. PCA separated Y10 from Y0 samples, and the volcano plot showed that most differential metabolites accumulated in Y10. The dominant metabolite classes included carboxylic acids and derivatives, benzenoids, fatty acyls, organooxygen compounds, organonitrogen compounds, and prenol lipids, while KEGG enrichment highlighted pathways related to microbial metabolism in diverse environments, aromatic compound degradation, alkaloid biosynthesis, sulfur metabolism, and indole alkaloid biosynthesis. Root exudates and rhizosphere metabolites can function as microbial substrates, signals, allelochemicals, or antimicrobial compounds, thereby shaping plant–soil feedbacks [10–12]. The enrichment of aromatic compound degradation pathways and secondary metabolite-related pathways in our study is consistent with the idea that continuous cropping changes both metabolite input and microbial metabolic demand in the rhizosphere.

Several key metabolites identified in enriched pathways, including DOPA, dictamnine, phenylacetaldehyde, benzaldehyde, 4-hydroxyphenyl acetate, allantoinic acid, and fumaric acid, may be relevant to the altered rhizosphere state. Phenolic and aromatic compounds are often involved in plant-microbe interactions and can influence microbial recruitment or inhibition [10,12]. In pepper, recent work has shown that the flavonoid apigenin can simultaneously suppress Phytophthora capsici and reshape the pepper microbiome, illustrating how specific metabolites may connect pathogen pressure and microbiome assembly [13]. Although our metabolomics data do not prove that the detected metabolites directly caused microbial shifts, the coordinated changes in metabolite profiles, KEGG pathways, and microbial communities suggest that metabolite-mediated selection may be an important component of pepper continuous cropping obstacles.

The microbial diversity results support this interpretation. Both bacterial and fungal richness and Shannon diversity were significantly reduced in Y10 soils, and PCoA revealed strong separation between Y0 and Y10 communities. Declines in microbial alpha diver-

sity and changes in beta diversity have been reported in hot pepper continuous-cropping soils [8], and reduced microbial diversity is often associated with lower functional redundancy and weaker resistance to soil-borne pathogens [4,5]. In our study, the reduction in fungal diversity was particularly pronounced, suggesting that fungal communities may be highly sensitive to the altered soil and metabolite environment caused by long-term pepper monoculture. This agrees with previous work showing that long-term continuous pepper cropping simplified fungal interaction networks and shifted fungal community composition [9].

At the taxonomic level, continuous cropping reorganized both bacterial and fungal communities. In bacteria, Y10 soils were enriched in Proteobacteria, Bacteroidota, Chloroflexi, Patescibacteria, and Firmicutes, whereas Y0 soils had higher relative abundances of Acidobacteriota, Nitrospirota, Myxococcota, and Methylomirabilota. The enrichment of Proteobacteria and Bacteroidota in Y10 may reflect a shift toward more copiotrophic or stress-responsive taxa under nutrient-rich and metabolite-rich rhizosphere conditions. In contrast, the reduction in *Nitrospirota* and several Y0-enriched genera such as *Nitrospira*, *RB41*, and *Bryobacter* may indicate weakened nitrification potential and loss of taxa associated with more stable soil environments. Previous studies on hot pepper also reported that continuous cropping changed bacterial diversity, community composition, and predicted functions related to nitrogen, phosphorus, energy, amino acid, and carbohydrate metabolism [8]. Thus, the bacterial community shift observed here is consistent with a transition from a diverse and functionally balanced rhizosphere toward a more disturbed and selectively filtered community.

The observed taxonomic shifts should be interpreted in the context of genus-level ecological potential rather than direct evidence of disease causation. For example, Pseudomonas and Bacillus include both beneficial and opportunistic members, whereas Fusarium, Alternaria, Aspergillus, Neocosmospora, and related fungal genera include species with diverse saprotrophic, endophytic, opportunistic, or pathogenic lifestyles. Because no pathogenicity assay, disease index, or yield assessment was included, the present data indicate community redistribution rather than confirmed pathogen accumulation.

Similarly, PICRUSt2 and FUNGuild results should be considered predictions of functional potential. These tools are useful for generating hypotheses about nutrient cycling, chemotaxis, transport, degradation pathways, and fungal trophic guilds, but the predicted functions require validation by metagenomics, metatranscriptomics, enzyme assays, isolation experiments, or targeted functional-gene quantification.

The metabolomic results further suggest that long-term monoculture was associated with broad changes in rhizosphere chemical composition, especially aromatic compounds, alkaloid-related metabolites, sulfur-related metabolites, and microbial-metabolism-related pathways. Because metabolite annotations in untargeted LC-MS are putative unless confirmed with authentic standards, the listed compounds should be treated as candidate markers for future targeted validation rather than definitive chemical diagnoses.

Taken together, our results support a conceptual model in which long-term pepper continuous cropping first alters the soil biochemical environment, particularly by decreasing pH and MBC while increasing EC and available nutrients. These changes are accompanied by the accumulation of differential rhizosphere metabolites, including aromatic and secondary-metabolism-related compounds, which may further impose selective pressure on microbial communities. Under this combined environmental and metabolic filtering, bacterial and fungal diversity decline, beneficial or functionally stable taxa are reduced, and potential pathogenic or opportunistic taxa become enriched. The resulting microbial community may have lower functional redundancy, altered nutrient-cycling capacity, and greater disease risk, thereby reinforcing continuous cropping obstacles.

Several limitations should be considered. First, the comparison involved two field conditions within a single demonstration base rather than independently replicated fields, so the results are best interpreted as an observational comparison of two cropping histories. Second, baseline soil conditions and complete historical records of fertilizer, pesticide, residue, liming, and tillage inputs were not available. Third, soil variables were measured with three biological replicates per group, whereas sequencing and metabolomics used six biological replicates per group; therefore, cross-omics correlations are exploratory. Fourth, yield, disease severity, root symptoms, pathogen isolation, and pathogenicity tests were not performed. Finally, functional predictions and metabolite annotations require experimental validation.

5. Conclusions

In conclusion, 10 years of pepper monoculture was associated with coordinated shifts in rhizosphere soil chemistry, enzyme activity, microbial diversity, microbial taxonomic composition, predicted functional potential, and metabolite profiles. Y10 soils showed lower pH, MBC, microbial diversity, and several mineral elements but higher OM, available nutrients, and EC in soil-water extracts. Bacterial and fungal communities shifted toward distinct genus-level taxa, and metabolomic profiles indicated extensive remodeling of aromatic, alkaloid-related, sulfur-related, and microbial-metabolism-associated compounds. These findings provide an integrated view of soil biochemical and microbial changes associated with long-term pepper monoculture and support future work on crop rotation, balanced fertilization, organic amendments, microbiome management, and targeted validation of microbial and metabolite indicators.

Supplementary Materials: The following supporting information can be downloaded at: https://www.mdpi.com/article/10.3390/agriculture16151663/s1.

Author Contributions: Conceptualization, Y.Z. (Yaxian Zhao) and Q.Y.; methodology, F.Y., Z.H. and Y.Z. (Ying Zhang); software, F.Y. and Z.H.; validation, Y.Z. (Ying Zhang), Q.Y. and Y.Z. (Yaxian Zhao); formal analysis, F.Y. and Z.H.; investigation, F.Y., Z.H., Y.Z. (Ying Zhang), X.W., Y.H., X.C. and W.Y.; resources, Y.Z. (Yaxian Zhao) and Q.Y.; data curation, F.Y. and Z.H.; writing—original draft preparation, F.Y. and Z.H.; writing—review and editing, Y.Z. (Yaxian Zhao), Q.Y., Y.Z. (Ying Zhang) and X.W.; visualization, F.Y.; supervision, Y.Z. (Yaxian Zhao) and Q.Y.; project administration, Q.Y.; funding acquisition, Q.Y. All authors have read and agreed to the published version of the manuscript.

Funding: This research was funded by the Henan Province Key Research and Development and Promotion Science and Technology Project, grant number 252102111094; the Key Research and Development Special Project of Henan Province, grant number 251111111100; the Henan Academy of Agricultural Sciences Independent Innovation Project, grant number 2026ZC112 and 2026ZC114; the Earmarked Fund for China Agriculture Research System, grant number CARS-22; and the Henan Academy of Agricultural Sciences Science and Technology Innovation Team Program, grant number 2024TD43.

Data Availability Statement: The raw sequencing data generated in this study have been deposited in the NCBI Sequence Read Archive (SRA) under BioProject accession number PRJNA1496486. The metabolomics datasets will be deposited in an appropriate public repository before final publication. During the review process, the metabolomics data are available from the corresponding author upon reasonable request. The corresponding repository accession numbers for metabolomics data will be added once available.

Conflicts of Interest: The authors declare no conflicts of interest.

References

1. Bennett, A.J.; Bending, G.D.; Chandler, D.; Hilton, S.; Mills, P. Meeting the Demand for Crop Production: The Challenge of Yield Decline in Crops Grown in Short Rotations. *Biol. Rev.* **2012**, *87*, 52–71. [CrossRef] [PubMed]
2. Chen, W.; Guo, X.; Guo, Q.; Tan, X.; Wang, Z. Long-Term Chili Monoculture Alters Environmental Variables Affecting the Dominant Microbial Community in Rhizosphere Soil. *Front. Microbiol.* **2021**, *12*, 681953. [CrossRef] [PubMed]
3. Yu, J.; Liu, Y.; Wang, Z.; Huang, X.; Chai, D.; Gu, Y.; Zhao, K.; Yu, X.; Shuai, Z.; Liu, H.; et al. The Cropping Obstacle of Garlic Was Associated with Changes in Soil Physicochemical Properties, Enzymatic Activities and Bacterial and Fungal Communities. *Front. Microbiol.* **2022**, *13*, 828196. [CrossRef] [PubMed]
4. Philippot, L.; Raaijmakers, J.M.; Lemanceau, P.; van der Putten, W.H. Going Back to the Roots: The Microbial Ecology of the Rhizosphere. *Nat. Rev. Microbiol.* **2013**, *11*, 789–799. [CrossRef] [PubMed]
5. Berendsen, R.L.; Pieterse, C.M.J.; Bakker, P.A.H.M. The Rhizosphere Microbiome and Plant Health. *Trends Plant Sci.* **2012**, *17*, 478–486. [CrossRef] [PubMed]
6. Burns, R.G.; DeForest, J.L.; Marxsen, J.; Sinsabaugh, R.L.; Stromberger, M.E.; Wallenstein, M.D.; Weintraub, M.N.; Zoppini, A. Soil Enzymes in a Changing Environment: Current Knowledge and Future Directions. *Soil Biol. Biochem.* **2013**, *58*, 216–234. [CrossRef]
7. Nannipieri, P.; Giagnoni, L.; Renella, G.; Puglisi, E.; Ceccanti, B.; Masciandaro, G.; Fornasier, F.; Moscatelli, M.C.; Marinari, S. Soil Enzymology: Classical and Molecular Approaches. *Biol. Fertil. Soils* **2012**, *48*, 743–762. [CrossRef]
8. Li, Y.; Liu, L.; Jiang, Y.; He, X.; Qiu, Y.; Ren, L.; Fu, J. Effect of Continuous Cropping of Hot Pepper on Soil Bacterial Community. *Acta Microbiol. Sin.* **2023**, *63*, 297–318. [CrossRef]
9. Chen, F.; Yu, G.; Wang, X.; Li, T.; Sun, Y. Response Characteristics of Soil Fungal Community Structure to Long-Term Continuous Cropping of Pepper. *Environ. Sci.* **2024**, *45*, 543–554. [CrossRef] [PubMed]
10. Bais, H.P.; Weir, T.L.; Perry, L.G.; Gilroy, S.; Vivanco, J.M. The Role of Root Exudates in Rhizosphere Interactions with Plants and Other Organisms. *Annu. Rev. Plant Biol.* **2006**, *57*, 233–266. [CrossRef] [PubMed]
11. Badri, D.V.; Vivanco, J.M. Regulation and Function of Root Exudates. *Plant Cell Environ.* **2009**, *32*, 666–681. [CrossRef]
12. Hu, L.; Robert, C.A.M.; Cadot, S.; Zhang, X.; Ye, M.; Li, B.; Manzo, D.; Chervet, N.; Steinger, T.; van der Heijden, M.G.A.; et al. Root Exudate Metabolites Drive Plant-Soil Feedbacks on Growth and Defense by Shaping the Rhizosphere Microbiota. *Nat. Commun.* **2018**, *9*, 2738. [CrossRef] [PubMed]
13. Liao, X.; Song, W.; Wan, Y.; Zhang, J.; Ren, P.; Delaplace, P.; Chen, Y. Dual Functions of Apigenin in Suppressing *Phytophthora capsici* and Shaping the Pepper Microbiome. *Microbiome* **2026**, *early access*. [CrossRef] [PubMed]
14. *HJ 615-2011*; Soil—Determination of Organic Carbon—Potassium Dichromate Oxidation Spectrophotometric Method. China Environmental Science Press: Beijing, China, 2011.
15. *NY/T 1121.6-2006*; Soil Testing—Part 6: Method for Determination of Soil Organic Matter. China Agriculture Press: Beijing, China, 2006.
16. *DB51/T 1975-2014*; Soil—Determination of Alkali-Hydrolyzable Nitrogen. Sichuan Provincial Bureau of Quality and Technical Supervision: Chengdu, China, 2014.
17. *NY/T 1121.2-2006*; Soil Testing—Part 2: Method for Determination of Soil pH. China Agriculture Press: Beijing, China, 2006.
18. *HJ 802-2016*; Soil—Determination of Electrical Conductivity—Electrode Method. China Environmental Science Press: Beijing, China, 2016.
19. *LY/T 1253-1999*; Forest Soil Analysis Methods. China Standards Press: Beijing, China, 1999.
20. *GB/T 17138-1997*; Soil Quality—Determination of Copper and Zinc—Flame Atomic Absorption Spectrophotometry. China Standards Press: Beijing, China, 1997.
21. *GB 17378.5-2007*; The Specification for Marine Monitoring—Part 5: Sediment Analysis. China Standards Press: Beijing, China, 2007.
22. Bolger, A.M.; Lohse, M.; Usadel, B. Trimmomatic: A Flexible Trimmer for Illumina Sequence Data. *Bioinformatics* **2014**, *30*, 2114–2120. [CrossRef] [PubMed]
23. Zhang, J.; Kobert, K.; Flouri, T.; Stamatakis, A. PEAR: A Fast and Accurate Illumina Paired-End reAd mergeR. *Bioinformatics* **2014**, *30*, 614–620. [CrossRef] [PubMed]
24. Magoč, T.; Salzberg, S.L. FLASH: Fast Length Adjustment of Short Reads to Improve Genome Assemblies. *Bioinformatics* **2011**, *27*, 2957–2963. [CrossRef] [PubMed]
25. Rognes, T.; Flouri, T.; Nichols, B.; Quince, C.; Mahé, F. VSEARCH: A Versatile Open Source Tool for Metagenomics. *PeerJ* **2016**, *4*, e2584. [CrossRef] [PubMed]
26. Edgar, R.C. UPARSE: Highly Accurate OTU Sequences from Microbial Amplicon Reads. *Nat. Methods* **2013**, *10*, 996–998. [CrossRef] [PubMed]
27. Quast, C.; Pruesse, E.; Yilmaz, P.; Gerken, J.; Schweer, T.; Yarza, P.; Peplies, J.; Glöckner, F.O. The SILVA Ribosomal RNA Gene Database Project: Improved Data Processing and Web-Based Tools. *Nucleic Acids Res.* **2013**, *41*, D590–D596. [CrossRef] [PubMed]

28. Nilsson, R.H.; Larsson, K.H.; Taylor, A.F.S.; Bengtsson-Palme, J.; Jeppesen, T.S.; Schigel, D.; Kennedy, P.; Picard, K.; Glöckner, F.O.; Tedersoo, L.; et al. The UNITE Database for Molecular Identification of Fungi: Handling Dark Taxa and Parallel Taxonomic Classifications. *Nucleic Acids Res.* **2019**, *47*, D259–D264. [CrossRef] [PubMed]
29. Parks, D.H.; Tyson, G.W.; Hugenholtz, P.; Beiko, R.G. STAMP: Statistical Analysis of Taxonomic and Functional Profiles. *Bioinformatics* **2014**, *30*, 3123–3124. [CrossRef] [PubMed]
30. Douglas, G.M.; Maffei, V.J.; Zaneveld, J.R.; Yurgel, S.N.; Brown, J.R.; Taylor, C.M.; Huttenhower, C.; Langille, M.G.I. PICRUSt2 for Prediction of Metagenome Functions. *Nat. Biotechnol.* **2020**, *38*, 685–688. [CrossRef] [PubMed]
31. Kanehisa, M.; Goto, S. KEGG: Kyoto Encyclopedia of Genes and Genomes. *Nucleic Acids Res.* **2000**, *28*, 27–30. [CrossRef] [PubMed]
32. Nguyen, N.H.; Song, Z.; Bates, S.T.; Branco, S.; Tedersoo, L.; Menke, J.; Schilling, J.S.; Kennedy, P.G. FUNGuild: An Open Annotation Tool for Parsing Fungal Community Datasets by Ecological Guild. *Fungal Ecol.* **2016**, *20*, 241–248. [CrossRef]
33. Kessner, D.; Chambers, M.; Burke, R.; Agus, D.; Mallick, P. ProteoWizard: Open Source Software for Rapid Proteomics Tools Development. *Bioinformatics* **2008**, *24*, 2534–2536. [CrossRef] [PubMed]
34. Smith, C.A.; Want, E.J.; O'Maille, G.; Abagyan, R.; Siuzdak, G. XCMS: Processing Mass Spectrometry Data for Metabolite Profiling Using Nonlinear Peak Alignment, Matching, and Identification. *Anal. Chem.* **2006**, *78*, 779–787. [CrossRef] [PubMed]
35. Shen, X.; Wang, R.; Xiong, X.; Yin, Y.; Cai, Y.; Ma, Z.; Liu, N.; Zhu, Z.J. Metabolic Reaction Network-Based Recursive Metabolite Annotation for Untargeted Metabolomics. *Nat. Commun.* **2019**, *10*, 1516. [CrossRef] [PubMed]
36. Wishart, D.S.; Guo, A.; Oler, E.; Wang, F.; Anjum, A.; Peters, H.; Dizon, R.; Sayeeda, Z.; Tian, S.; Lee, B.L.; et al. HMDB 5.0: The Human Metabolome Database for 2022. *Nucleic Acids Res.* **2022**, *50*, D622–D631. [CrossRef] [PubMed]
37. R Core Team. *R: A Language and Environment for Statistical Computing*; R Foundation for Statistical Computing: Vienna, Austria, 2024.
38. Wickham, H. *Ggplot2: Elegant Graphics for Data Analysis*, 2nd ed.; Springer: Cham, Switzerland, 2016. [CrossRef]